Journal of Photochemistry and Photobiology A: Chemistry 198 (2008) 7–12

Contents lists available at ScienceDirect

Journal of Photochemistry and Photobiology A: Chemistry

journal homepage: www.elsevier.com/locate/jphotochem

Interaction of water-soluble thiol capped CdTe quantum dots and bovine serum albumin

Mopelola Idowu, Emmanuel Lamprecht, Tebello Nyokong*

Department of Chemistry, Rhodes University, Grahamstown 6140, South Africa

ARTICLE INFO

Article history:
Received 10 October 2007
Received in revised form 3 December 2007
Accepted 10 February 2008
Available online 15 February 2008

Keywords:
Quantum Dots
Bovine serum albumin
Cysteine
Thioglycolic acid
Mercaptopropionic acid
Cadmium tellurium

ABSTRACT

Luminescent water-soluble CdTe quantum dots (QDs) capped with different thiol carboxylic acids were synthesized in aqueous medium and then cross linked to bovine serum albumin (BSA) with 1-ethyl-3-(3-dimethylaminopropyl) carbodiimide hydrochloride (EDC). Enhancement of fluorescence emission intensity occurred for QDs in the presence of bovine serum albumin (BSA, mixed or linked) signifying inhibition of non-radiative recombination of the surface vacancies. Fluorescence studies reveal a positive deviation behaviour suggesting the occurrence of static and dynamic mechanisms of quenching together which was accounted for by the modified Stern–Volmer equation.

1. Introduction

Quantum dots (QDs) have gained a lot of attention in the past decade. The quantum confinement of their electronic states makes them quite attractive, showing some unique optical properties such as high quantum yield, symmetrical emission spectra, broad-band excitation, photostability, and readily tunable spectra [1–4] compared to conventional dyes.

QDs and their molecular conjugates are becoming increasingly important for a wide range of applications in biotechnology, and medicine [5–12]. Silica and metal nanoparticles [13–15] have been applied for detection of proteins and for clinical diagnosis but the use of QDs in imaging and as phototherapeutic agents is becoming common.

Bovine serum albumin (BSA) is the most studied protein having a high percentage of the total plasma protein. Serum albumins play an important role in the transport of many exogenous and endogenous ligands, binding covalently or reversibly to these ligands and increasing the tumor selectivity of the ligands by enhanced permeation and retention effect [16–19]. Therefore, binding of ligands to serum albumin is an important determinant of their distribution and fate in the body [20]. BSA has been widely used in this regard [21,22] due to its unusual binding properties [23].

The interaction of cadmium sulphide (CdS) quantum dots with BSA has been studied in reverse micelles [24] due to the insolubility of CdS QDs in aqueous medium. However, for cell applications, water solubility is necessary, so, it is desirable to study the interaction of BSA with water-soluble CdTe QDs capped with carboxylic thiols. Studying the interaction of CdTe quantum dots with BSA in aqueous medium, will give a representative model of the effect of CdTe QDs on cells in *in vivo* studies. Chemically reduced BSA has been employed to modify the surface of QDs [25,26]. Such denatured BSA conjugates to the surface of the CdTe QDs, improving their chemical stability and photolumiscence [26]. The improvement in the latter could lead to an increase in applications of the QDs such as in fluorescence imaging and other biological applications such as pathogen and toxin detection [27]. The current work aims at studying the effect of BSA on QDs without prior chemical reduction of the former.

Also, having a crosslinker between BSA and CdTe QDs will give an understanding of the capabilities of biomolecules–QDs coupling techniques. Bifunctional reagents like glutaraldehyde has been widely used in crosslinking of biomaterials, however, a negative effect on their biocompatibility can hardly be avoided [28]. Ethyl-3-(3-dimethylaminopropyl) carbodiimide hydrochloride (EDC) [27,29,30] has been found to be comparable to glutaraldehyde as a crosslinker, hence, our choice of EDC as a coupling agent for the coordination of CdTe QDs (through carboxylic acid groups) to the amino group of BSA.

In this work, we report on the spectroscopic investigation of the interaction of water-soluble CdTe quantum dots with

* Corresponding author. Tel.: + 27 46 6038260; fax: +27 46 6225109.
E-mail address: t.nyokong@ru.ac.za (T. Nyokong).

1010-6030/$ – see front matter © 2008 Elsevier B.V. All rights reserved.
doi:10.1016/j.jphotochem.2008.02.008

BSA. The effect of QDs on the BSA fluorescence quenching was investigated.

2. Experimental

2.1. Materials

$CdCl_2{\cdot}H_2O$, tellurium powder (200 mesh), thioglycolic acid, 3-mercaptopropionic acid, L-cysteine, bovine serum albumin, 1-ethyl-3-(3-dimethylaminopropyl) carbodiimide hydrochloride (EDC) and Rhodamine 6G were obtained from Sigma–Aldrich. $NaBH_4$, NaOH and H_2SO_4 were obtained from SAARCHEM. Ultra pure water was obtained from a Milli-Q Water System (Millipore Corp., Bedford, MA, USA). Phosphate buffer saline (PBS) solution (0.01 M, pH 7.4) was employed.

2.2. Synthesis of quantum dots

The preparation of thiol capped QD was via a modified method adopted from literature [31,32]. Briefly, 2.35 mmol of $CdCl_2{\cdot}H_2O$ was dissolved in 125 ml of water and 5.7 mmol of the respective carboxylic thiol (thioglycolic acid (TGA), 3-mercaptopropionic acid (MPA) or L-cysteine (CYS)) was added under stirring. The solution was adjusted to pH 12 with 1 M NaOH. Nitrogen gas was bubbled through the solution for about 1 h. The aqueous solution was reacted with H_2Te gas. H_2Te gas being generated by the reaction of $NaBH_4$ with Te powder in the presence of 0.5 M H_2SO_4 under a flow of nitrogen gas. A change of colour of the solution containing $CdCl_2$ and the thiol was observed on addition of H_2Te gas. The solution was then refluxed under air at 100 °C for different times to control the size of the CdTe QDs. On cooling, the QDs were precipitated out from solution using excess ethanol; the solutions were then centrifuged to harvest the QDs. The structures of the thiols (thioglycolic acid (TGA), 3-mercaptopropionic acid (MPA) and L-cysteine (CYS)) used to cap QDs are shown in Fig. 1 (Inset). The synthesized QDs are: (i) MPA capped CdTe with emission peak at 550 nm (QD (MPA)), (ii) TGA capped CdTe with emission peak at 587 nm (QD (TGA)) and (iii) CYS capped CdTe with emission peak at 567 nm (QD (CYS)).

2.3. Conjugation of CdTe QDs to BSA

Carboxylic thiol capped CdTe QDs were linked to BSA using EDC as a crosslinker in aqueous medium (PBS pH 7.4). Briefly, 3×10^{-7} M CdTe QDs and 1.04×10^{-5} M EDC were reacted together for 5 min at room temperature to allow for activation of the carboxylic end of the QDs, then; 3×10^{-6} M BSA was added into the reaction mixture and incubated for 2 h. Under the same conditions, a mixture of the CdTe QDs solution and BSA without EDC was made as a control experiment.

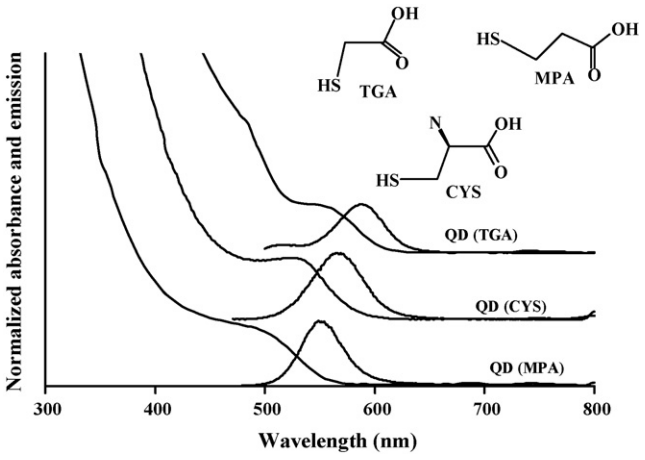

Fig. 1. Absorption and Emission spectra of CdTe quantum dots capped with different thiol carboxylic acids. QD (CYS): L-cysteine; QD (MPA): 3-mercaptopropionic acid and QD (TGA): thioglycolic acid capped CdTe QDs. Inset shows molecular structures of carboxylic thiol–ligands used in capping CdTe quantum dots.

2.4. Equipment

Fluorescence excitation and emission spectra were recorded on a Varian Eclipse spectrofluoremeter. UV–visible spectra were recorded on a Varian 500UV–Vis/NIR spectrophotometer. X-ray powder diffraction patterns were recorded on a Phillips PW1050 goniometer equipped with a proportional counter, using Cu Kα radiation ($\lambda = 1.5405$ Å, nickel filter). Data were collected in the range from $2\theta = 5^\circ$ to 60°, scanning at 1 min^{-1} with a filter time-constant of 1 s. Samples were placed on a glass slide, on a thin layer of petroleum grease where necessary, and a paper spacer was placed between the slide and the goniometer head to compensate for the thickness of the grease layer. The X-ray diffraction data were treated using the freely-available Fityk curve fitting software. Baseline correction was performed on each diffraction pattern by subtracting a spline fitted to the curved background, the control points having been selected manually by inspection. Pearson7-type curves were fitted to the raw data, having been found to provide the best fit, and the full-width at half-maximum values used in this study were obtained from the fitted curves. IR spectra were recorded on a Perkin–Elmer spectrum 2000 FTIR spectrometer.

2.5. Fluorescence studies

Fluorescence quantum yields (Φ_F) were determined by comparative method [33] using Eq. (1),

$$\Phi_F = \Phi_{F(R)} \frac{FA_R n^2}{F_R A n_R^2} \quad (1)$$

where F is the area under the fluorescence curves, A is the optical density at the excitation wavelength, and n is the refractive index of the solvent used. R refers to the reference fluorophore with known quantum yield. Rhodamine 6G with $\Phi_F = 0.94$ [34,35] in ethanol was employed as the standard. Φ_F was determined for both QDs and BSA in aqueous medium (pH 7.4 buffer). At least three independent experiments were performed for the quantum yield determinations. Both the sample and the reference were excited at the same relevant wavelength.

The determined fluorescence quantum yield values of QDs and BSA were employed in determining the fluorescence quantum yields of BSA and QD in each mixture ($\Phi^{Mix}_{F(BSA)}$ and $\Phi^{Mix}_{F(QD)}$) and in the linked form ($\Phi^{Linked}_{F(BSA)}$ and $\Phi^{Linked}_{F(QD)}$) using a modified form of Eq. (1) as shown by Eq. (2a) and (2b).

$$\Phi^{Mix}_{F(QD)} = \Phi_{F(QD)} \frac{F_{QD-BSA}}{F_{QD}} \quad (2a)$$

where $\Phi_{F(QD)}$ is the fluorescence quantum yield of the QDs alone, and was used as standard, F_{QD-BSA} is the fluorescence intensity of the QD in the mixture and F_{QD} is the fluorescence intensity of the QD alone. Excitations were done at 450 nm.

$$\Phi^{Mix}_{F(BSA)} = \Phi_{F(BSA)} \frac{F_{BSA-QD}}{F_{BSA}} \quad (2b)$$

where $\Phi_{F(BSA)}$ is the fluorescence quantum yield of the BSA alone, and was used as standard, F_{BSA-QD} is the fluorescence intensity of the BSA in the mixture and F_{BSA} is the fluorescence intensity of the BSA alone. Excitations were done at 280 nm.

Table 1
Spectral properties of thiol capped CdTe quantum dots (pH 7.4 PBS buffer)

Capping thiol[a]	Size (nm)	Absorption maxima (nm)	Emission (max) (nm)	Band gap (eV)	FWHM[b] (nm)
MPA	2.3	500	550	2.25	49
CYS	3.0	530	567	2.17	54
TGA	3.2	550	587	2.11	59

[a] CYS: L-cysteine; MPA: 3-mercaptopropionic acid and TGA: thioglycolic acid.
[b] FWHM: full-width at half maximum (FWHM).

The $\Phi^{\text{Linked}}_{F(\text{BSA})}$ and $\Phi^{\text{Linked}}_{F(\text{QD})}$ were determined in the same manner except the mixed forms, ($\Phi^{\text{Mix}}_{F(\text{BSA})}$ and $\Phi^{\text{Mix}}_{F(\text{QD})}$) were replaced by the linked forms ($\Phi^{\text{Linked}}_{F(\text{BSA})}$ and $\Phi^{\text{Linked}}_{F(\text{QD})}$) in Eq. (2).

2.6. Interaction of BSA with QD

The interaction of the BSA with QDs was studied by spectrofluorometry at room temperature. An aqueous solution of BSA (fixed concentration 3.0×10^{-6} M) was titrated with increasing concentrations (0 to 9.7×10^{-7} M) of the respective QD solution. BSA was excited at 280 nm and fluorescence spectra recorded between 290 nm and 500 nm. The steady decrease in the intrinsic fluorescence of tryptophan residues in BSA was noted and related to QDs concentration by the Stern–Volmer's plot [36] (Eq. (3)):

$$\frac{F_0}{F} = 1 + K_{\text{SV}}[\text{QD}] \tag{3}$$

where F_0 and F are the fluorescence intensities of BSA in the absence and presence of the QDs, respectively. QD is the concentration of the respective QDs and K_{sv} is the Stern–Volmer constant. The ratios F_o/F were calculated and plotted against QD according to Eq. (3).

3. Results and discussion

3.1. Spectral characterization of CdTe quantum dots

Typical normalized absorption and photoluminescence spectra of the synthesized quantum dots stabilized with different carboxylic thiol derivatives are shown in Fig. 1. The synthesized QDs are represented after the capping thiols as QD (CYS), QD (MPA), and QD (TGA). The absorption spectra of the QDs show typical broad peaks in the visible region with tails extending to about 700 nm similar to those previously reported for thiol stabilized CdTe QDs [9,31]. The absorption spectra of the synthesized QDs indicate that the CdTe QDs have a wide range of absorption with their absorption peak maxima ranging from 500 nm to 550 nm as shown in Fig. 1 (and Table 1). The absorbance maxima are well resolved, inferring narrow size distribution of the synthesized QDs.

The emission spectra of the QDs, overlaid with the absorption spectra in Fig. 1, were measured from prepared QDs solution diluted with water to absorbance of ~0.05 (at the excitation wavelength, 450 nm) appropriate for emission studies. The emission spectra are characterized by good symmetry, and are sufficiently narrow with full width at half maximum (FWHM) ranging from 49 nm to 59 nm as shown in Table 1 for the different QDs. The QDs are photoluminescent in the visible region with maxima ranging from 550 nm to 587 nm, Table 1. The size of the quantum dots increase with increase in reaction time resulting in shift in emission spectra to the red. Stokes shift ranged from 37 nm to 50 nm for the QDs in Table 1. Their band gap energies further proves the quantum confinement effect in QDs.

X-ray powder diffraction (XRPD) can provide information both about the crystal-structure and nanocrystalline properties of the QDs. Fig. 2 shows the X-ray diffraction patterns of the synthesized CdTe QD nanoparticles. The diffraction peaks are broad and weak, but the main peaks centred at approximately $2\theta = 25^\circ$, 40° and 47° correspond well to the three most intense peaks for bulk CdTe (ZnS-type structure, $2\theta = 23.8^\circ$, 39.3°, and 46.5°) as they appear on the simulated pattern obtained from crystal structure data using PLATON [37]. Following literature methods [38], the particle-diameter d, was estimated using the Scherrer Eq. (4):

$$d(\overset{o}{A}) = \frac{k\lambda}{\beta \operatorname{Cos}\theta} \tag{4}$$

where k is an empirical constant equal to 0.9, λ is the wavelength of the X-ray source, (1.5405 Å), β is the full width at half maximum of the diffraction peak, and θ is the angular position of the peak. The particle-sizes determined by XRPD, using the peak at 25°, were 2.2 nm, 2.7 nm and 2.2 nm, for QDs capped with MPA, CYS and TGA, respectively. The values for the MPA- and CYS-capped QDs are in reasonable agreement with the particle-sizes obtained by polynomial fitting function, Eq (5) [39].

$$D = (9.8127 \times 10^{-7})\lambda^3 - (1.7147 \times 10^{-3})\lambda^2 + (1.0064)\lambda - (194.84) \tag{5}$$

Using this polynomial fitting, the particle sizes were 2.3 nm (MPA), 3.0 nm (CYS) and 3.2 nm (TGA). Thus the value of the TGA-capped thiol is much smaller when determined by the XPRD method compared to estimation by the polynomial fitting.

3.2. Conjugation of CdTe QDs to BSA

The thiol groups located on the surface of CdTe QDs were linked to BSA by coordination of the carboxylic group of the thiol with the amine group on BSA. EDC was used to activate the carboxylic acid group of the thiol capping the QDs to facilitate linking with the amine group of BSA, Scheme 1. The intensity of QDs emission peaks

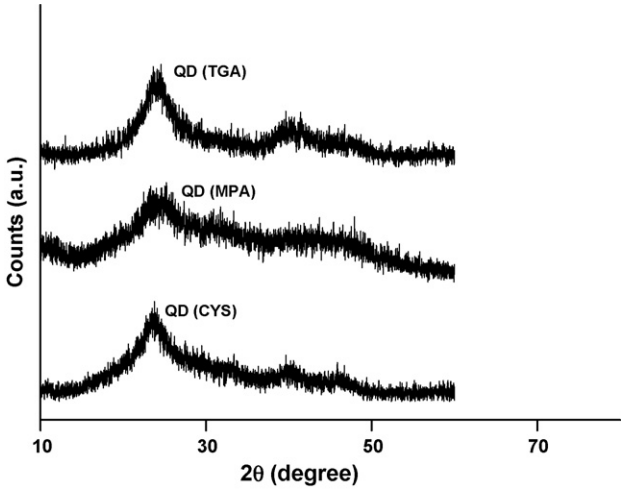

Fig. 2. X-ray diffractograms of the different thiol carboxylic acid stabilized CdTe quantum dots samples.

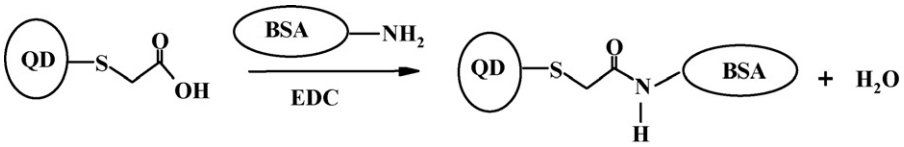

Scheme 1. BSA and QD linking process. QD: Quantum dots, BSA: Bovine serum albumin.

(excitation 280 nm) during the EDC activated coupling of CdTe QDs to BSA was monitored at fixed time intervals of 10 minutes each. The intensity of emission peaks of the QDs increased with time with all the QDs and then slowed or decreased slightly after 120 min Fig. 3. Thus all the data reported in this work was for QDs–BSA conjugates with a reaction time of 120 min. This time is a compromise between optimum formation of the conjugate and length of synthesis.

The increase in emission intensity of QDs observed in Fig. 3 may be due to the fact that the interaction of QDs with BSA passivates the surface of QDs and inhibits the radiationless recombination at the surface vacancies as it has been discussed before [40] and this kind of interaction is very useful in enhancing fluorescence intensity.

To establish our assumption of the formation of a link (amide bond), between the QDs and BSA, IR spectroscopy was carried out. In the linked QD–BSA form, there was an indication of an amide bond with the band at 3400 cm^{-1} (ν_{NH} (CONH)), while the mixed form showed a broad-band around 3300 cm^{-1}. Characteristic amide band was also observed at 1654 cm^{-1} in the linked, but this was not observed in the mixed where there is no amide bond.

3.3. Emission spectra of the interaction between CdTe QDs and BSA

Fig. 4 compares the absorption spectra of the BSA–QDs conjugates (linked or mixed) with that of QDs or BSA alone. There was a small decrease in the intensity of the QDs absorption on linking to BSA which was not observed in the mixture. In the emission spectra, a shift occurred in the wavelength of the QDs both in the mixture of CdTe QDs with BSA (Fig. 5, curves (iii) and CdTe QDs linked to BSA (Fig. 5, curves (iv) with excitation at 280 or 450 nm. Excitation at 280 nm, excites both BSA and QDs, however, this does not affect BSA emission since QDs emission is observed at much longer wavelengths. Fig. 5 shows that the shift in emission of QDs in the presence of BSA was to shorter wavelength while for the linked, there was a shift to longer wavelength. The blue shift in the emission maximum of QDs has been documented before in the interaction of QDs with silica coatings on its surface [41] and was explained to be due to the corrosion of the QDs during deposition on its surface. The blue shift in spectra was also reported when denatured BSA was used to modify the surface of CdTe QDs [26] and was explained in terms of possible shell of CdTe-BSA which leads to decrease in the CdTe inner core. The blue shift was also observed on excitation at 450 nm, Fig. 5a (inset). On the other hand, the red shift observed for the linked may be a result of amide bond formation as against corrosion (removal of QDs surface ligands) in the mixture of QDs and BSA. An increase in the emission intensity of QDs in a mixture (or linked) compared to equimolar concentration of QDs alone was observed in Fig. 5 on excitation at 280 nm (where both BSA and QDs absorb). However, this increase was also observed on excitation of the mixture (or linked complex) at the QDs wavelength only, i.e. at 450 nm excitation, Fig. 5a (inset), suggesting that the increase is not due to energy transfer from BSA to QDs. The enhancement in the photoluminescence of QDs in the presence of BSA has also been reported before [42] and used in the quantification of BSA. The concentration of BSA–QDs conjugate was kept the same as that of BSA alone or BSA in a mixture. The increase in intensity of the QDs emission in the presence of BSA could be due to passivation of the surface of QDs by BSA which increases fluorescence intensity as discussed above.

There was a complete collapse of the emission intensity of BSA in the presence of QDs on exciting at 280 nm (hence exciting both BSA and QDs), for QD (MPA) and QD (TGA) and a large reduction in intensity for QD (CYS), Fig. 5. The decrease (or complete disappearance) in BSA emission in the presence of QDs could be due to radiationless quenching of BSA fluorescence by QDs.

3.4. Fluorescence quenching of BSA by QDs

An efficient overlap between the absorption spectrum of the QDs with the emission spectra of BSA, (Fig. 6), was observed. This would normally be associated with a good energy transfer between the donor (BSA) and the acceptor (QDs). However, as stated above, there was no evidence that the increase in intensity of the

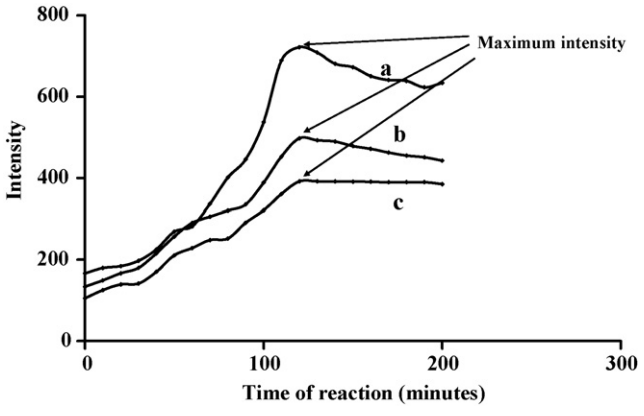

Fig. 3. Effect of time on conjugate formation: (a) QD (TGA); (b) QD (MPA); (c) QD (CYS). Excitation wavelength =280 nm.

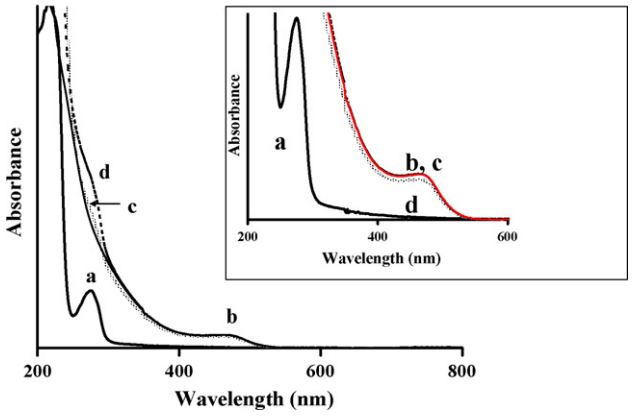

Fig. 4. UV–Vis absorption spectra of (a) BSA alone, (b) QD (MPA) alone, (c) QD (MPA) and BSA mixed and (d) QD (MPA) and BSA (linked). ([QD (MPA)] = 3×10^{-7} M; [BSA] = 3×10^{-6} M). Inset shows absorbance spectra in the 500 nm region enlarged.

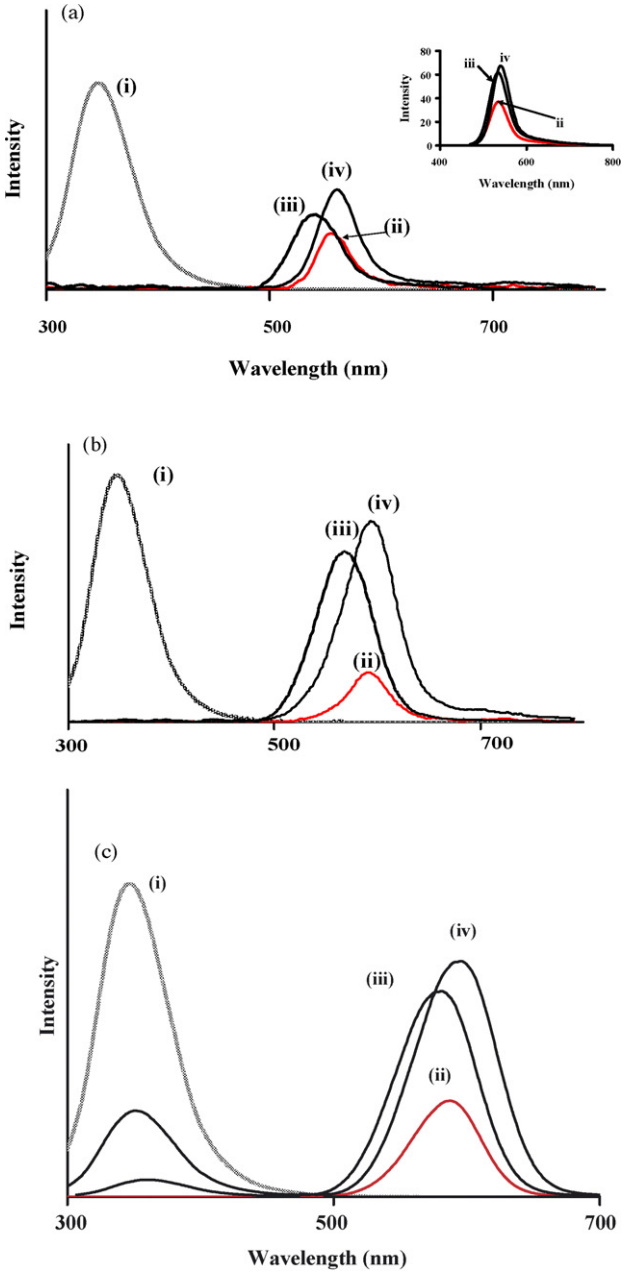

Fig. 5. Fluorescence spectra of (i) BSA, (ii) CdTe QD, (iii) BSA + CdTe QD and (iv) BSA + CdTe QD + EDC. Excitation wavelength =280 nm. [QD] = 3×10^{-7} M [BSA] = 3×10^{-6} M kept constant for all experiments. (a) QD (MPA), (b) QD (TGA) and (c) QD (CYS). Inset in (a) shows (ii), (iii), and (iv) QD (MPA) at excitation of 450 nm.

emission of QDs in the presence of BSA is due to energy transfer.

Fluorescence quantum yield (Φ_F) values for the CdTe QDs alone were calculated using Eq. (1) and listed in Table 2. The QDs have relatively high quantum yields compared to conventional dyes with QD (MPA) having the lowest Φ_F of 0.19. There is some correlation between the Φ_F and the sizes of the QDs in Table 2, since the QDs with the highest Φ_F are also one of the large ones. The differences in Φ_F values for the QDs may be ascribed to the structural differences in the different cappings used.

Fluorescence quantum yields of the QDs and BSA ($\Phi^{\text{Mix}}_{F(\text{QD})}$ and $\Phi^{\text{Mix}}_{F(\text{BSA})}$) in the mixture and the linked form ($\Phi^{\text{Linked}}_{F(\text{QD})}$ and $\Phi^{\text{Linked}}_{F(\text{BSA})}$) were determined using (Eq. (2a) and (2b)). Excitation at 280 nm,

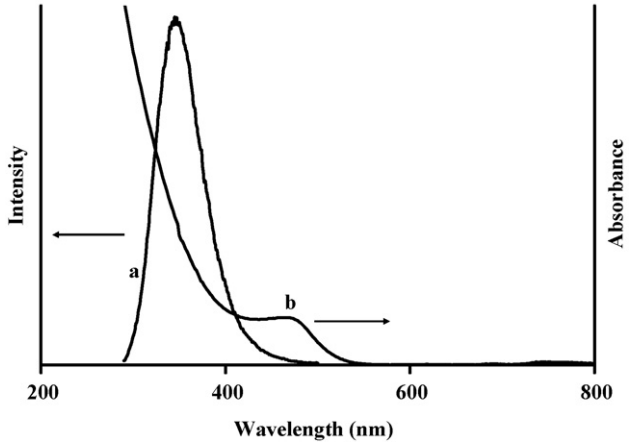

Fig. 6. Spectral overlap of (a) BSA fluorescence emission with (b) QD (MPA) absorption.

Table 2
Fluorescence quantum yields of QDs[a] and BSA in the mixed and linked forms, pH 7.4 PBS buffer

Capping[b] thiol	[c] $\Phi_{F(\text{QD})}$	$\Phi^{\text{Mix}}_{F(\text{QD})}$	$\Phi^{\text{Linked}}_{F(\text{QD})}$	$\Phi^{\text{Mix}}_{F(\text{BSA})}$	$\Phi^{\text{Linked}}_{F(\text{BSA})}$
MPA	0.19	0.20	0.22	0.009	0.0015
CYS	0.41	0.58	0.64	0.032	0.0064
TGA	0.30	0.69	0.82	0.007	0.0012

[a] $\Phi_{F(\text{QD})}$: Fluorescence quantum yield of QDs alone; $\Phi^{\text{Mix}}_{F(\text{QD})}$: fluorescence quantum yield of QD in the mixture with BSA, λ_{exc} = 450 nm; $\Phi^{\text{Linked}}_{F(\text{QD})}$: fluorescence quantum yield of QD when linked with BSA, λ_{exc} = 450 nm; $\Phi^{\text{Mix}}_{F(\text{BSA})}$: fluorescence quantum yield of BSA in the mixture with QD (λ_{exc} = 280 nm); $\Phi^{\text{Linked}}_{F(\text{BSA})}$: fluorescence quantum yield of BSA when linked with QD (λ_{exc} = 280 nm).

[b] CYS: L-cysteine; MPA: 3-mercaptopropionic acid and TGA: thioglycolic acid.

[c] $\Phi_{F(\text{BSA})}$ = 0.118 [44].

excites both BSA and QDs, however, BSA and QDs emit at different wavelengths. Hence the fluorescence quantum yields determined in the mixture and linked for BSA are not affected by QDs emission. Table 2 shows there is a decrease in $\Phi^{\text{Mix}}_{F(\text{BSA})}$ and $\Phi^{\text{Linked}}_{F(\text{BSA})}$ for all the conjugates compared to $\Phi_{F(\text{BSA})}$ of BSA alone, indicating the interaction occurring between the QDs and BSA results in quenching of the fluorescence of the latter. There was an increase in $\Phi^{\text{Mix}}_{F(\text{QD})}$ and $\Phi^{\text{Linked}}_{F(\text{QD})}$ (Table 2) compared to $\Phi_{F(\text{QD})}$ of the respective QDs. The error in Φ_F values shown in Table 2 is ±10%.

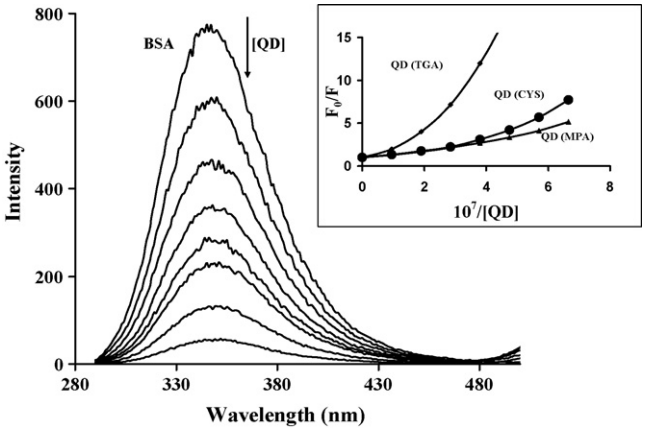

Fig. 7. Change in fluorescence intensity of BSA with QD (MPA). [QD (MPA)] = 0–9.7 × 10^{-7}, [BSA] = 3 × 10^{-6} M. Inset shows positive deviation from expected Stern–Volmer's plot for BSA quenching by increasing [QD].

Table 3
Quenching parameters for BSA–QD interactions in pH 7.4 PBS buffer

Capping thiol[a]	Ksv ($10^{-6}M^{-1}$)	Ka ($10^{-6}M^{-1}$)	Ks ($10^{-6}M^{-1}$)
MPA	1.20	7.22	2.11
CYS	1.79	12.2	3.55
TGA	2.84	27.7	8.41

[a] CYS: L-cysteine; MPA: 3-mercaptopropionic acid and TGA: thioglycolic acid.

Fig. 7 shows the fluorescence emission spectra of BSA (3.0×10^{-6} M) in the presence of varying concentrations (0–9.7×10^{-7} M) of the QD (MPA). BSA's fluorescence was found to decrease progressively with increasing concentration of QDs. This was also observed for all the other QDs. A positive deviation (with a concave towards the *y* axis) Fig. 7 inset from the Stern–Volmer's relationship was observed from the plot of F_0/F against [QD] for the quenching of BSA's fluorescence with QD, within investigated range of concentrations, suggesting that static and dynamic quenching may be occurring together. In order to accommodate both types of quenching, a modified Stern–Volmer's equation, Eq. (6) [34,43], which has been derived before is introduced. The deviation allows for an additional term to be introduced into the Stern–Volmer's equation.

$$\frac{F_0}{F} = (1 + K_{SV}[QD])(1 + K_a[QD]) \quad (6)$$

The first term is the original Stern–Volmer's equation, Eq. (3), which accounts for the dynamic quenching, the second term accounts for the upward curvature (static quenching). The quenching constant for the second term (K_a) is termed association constant. To solve for K_a, apparent values of K_{sv} (K_{app}) were calculated at each quencher (QD) concentration using Eq. (3), plotted against [QD] and extrapolated to [QD] =0 to obtain K_{sv}. Plotting $F_0/F(1 + K_{sv}[QD])$ against [QD] (figure not shown), gave K_a, according to Eq. (6).

K_{sv} and K_a values were quite high as listed in Table 3 with QD (TGA) having the highest values; this may explain why the rate of quenching is quite high in these samples. K_{sv} and K_a decreased in the order QD (TGA) > QD (CYS) > QD (MPA). MPA QDs are smaller in size hence resulting in lower values of the constants. The lack of shift in the absorption spectra of the QDs in the presence of BSA (Fig. 4) suggests that there is no significant association between the QDs and BSA in the ground state, and that the static component of the interaction of BSA with the QDs is from close proximity of the QD and BSA at the moment of excitation. This type of apparent static quenching constant (K_s) value is usually determined by plotting ln $(F_0/F(1 + K_{sv}[QD])$ against [QD] which is a modified Stern–Volmer's plot [34,43]. K_s values from the plot are listed in Table 3 and they represent the apparent quenching constant due to interaction of the fluorophore (BSA) and quencher (QD) at the excited state.

4. Conclusions

Luminescent CdTe (QDs) were synthesized in aqueous medium and conveniently cross linked to BSA. Emission enhancement was observed in the QDs when in the mixture with BSA or when linked due to radiationless recombination at the surface vacancies. A positive deviation from linearity of the Stern–Volmer plots in the quenching studies was attributed to dynamic and static mechanisms of quenching occurring together.

Acknowledgements

This work was supported by Rhodes University and the National Research Foundation (NRF GUN 2053657) of South Africa.

References

[1] M.B.M. Moronne Jr., P. Gin, S. Weiss, A.P. Alivisatos, Science 281 (1998) 2013.
[2] W.C.W. Chan, S. Nie, Science 281 (1998) 2016.
[3] F.X. Wu, J.W. Lewis, D.S. Kliger, J.Z. Zhang, J. Chem. Phys. 118 (2003) 12.
[4] X.H. Zhong, Y.Y. Feng, W. Knoll, M.Y. Han, J. Am. Chem. Soc. 125 (2003) 13559.
[5] A.P. Alivasatos, Science 271 (1996) 933.
[6] A.P. Alivasatos, J. Phys. Chem. 100 (1996) 13226.
[7] N. Gaponik, I.L. Radtchenko, G.B. Sukhorukov, H. Weller, A.L. Rogach, Adv. Mater. 14 (2002) 879.
[8] M. Han, X. Gao, J.Z. Su, S. Nie, Nat. Biotechnol. 19 (2001) 631.
[9] D.V. Talapin, A.L. Rogach, E.V. Shevchenko, A. Komowski, M. Haase, H. Weller, J. Am. Chem. Soc. 124 (2002) 5782.
[10] H. Mattoussi, J.M. Mauro, E.R. Goldman, G.P. Anderson, V.C. Sundar, F.V. Mikulec, M.G. Bawendi, J. Am. Chem. Soc. 122 (2000) 12142.
[11] A.C.S. Samia, S. Dayal, C. Burda, Photochem. Photobiol. 82 (2006)617.
[12] A.C.S. Samia, X. Chen, C. Burda, J. Am. Chem. Soc. 125 (2003) 15736.
[13] S. Santra, P. Zhang, K. Wang, R. Tapec, W. Tan, Anal. Chem. 73 (2001) 4988.
[14] M. Qhobosheane, S. Santra, P. Zhang, W. Tan, Analyst 126 (2001) 1274.
[15] R. Elghanian, J.J. Storhoff, R.C. Mucic, R.L. Letsinger, C.A. Mirkin, Science 277 (1997) 1078.
[16] U. Kragh-Hansen, Pharmacol. Rev. 33 (1981) 17.
[17] T. Tanaka, S. Shiramoto, M. Miyashita, Y. Fujishima, Y. Kaneo, Int. J. Pharmaceut. 277 (2004) 39.
[18] D.C. Carter, J.X. Ho, Adv. Protein Chem. 45 (1994) 153.
[19] A.K. Bordbar, A. Eslami, S. Tangestaninejad, J. Porphyrins Phthalocya. 6 (2002) 225.
[20] A.A. Bhattacharya, S. Curry, N.P. Franks, J. Biol. Chem. 275 (2000) 38731.
[21] D. Silva, C.M. Cortez, S.R.W. Louro, Braz. J. Med. Biol. Res. 37 (2004)963.
[22] E.L. Gelamo, M. Tabak, Spectrochim. Acta 56 (2000) 2255.
[23] D.C. Carter, B. Chang, J.X. Ho, K. Keeling, Z. Krishnasami, Eur. J. Biochem. 226 (1994) 1049.
[24] L. Tan, L.Y. Liu, Q. Xie, Y.Y. Zhang, S.Z. Yao, Anal. Sci. 20 (2004) 441.
[25] J.H. Wang, H.Q. Wang, H.L. Zhang, X.Q. Li, X.F. Hua, Y.C. Cao, Z.L. Huang, Y.D. Zhao, Anal. Bioanal. Chem. 388 (2007) 969.
[26] Q. Wang, Y. Kuo, Y. Wang, G. Shin, C. Ruengruglikit, Q. Huang, J. Phys. Chem. B 110 (2006) 16860.
[27] T. Jamieson, R. Bakhshi, D. Petrova, R. Pocock, M. Imani, A.M. Seifalian, Biomaterials 28 (2007) 4717.
[28] M. Grimm, E. Eybl, M. Grabenwoger, H. Spreitzer, W. Jager, G. Grimm, P. Bock, M.M. Muller, E. Wolner, Surgery 111 (1992) 74.
[29] L.H.H. Olde Damink, P.J. Dijkstra, M.J.A. vanLuyn, P.B. VanWachem, P. Nieuwnhuis, J. Feijen, Biomaterials 17 (1996) 679.
[30] C.S. Osborn, W.H. Reid, M.H. Grant, Biomaterials 20 (1999) 283.
[31] N. Gaponik, D.V. Talapin, A.L. Rogach, K. Hoppe, E.V. Shevchenko, A. Kornowski, A. Eychmuller, H. Weller, J. Phys. Chem. B 106 (2002) 7177.
[32] A. Shavel, N. Gaponik, A. Eychmuller, J. Phys. Chem. B 110 (2006) 19280.
[33] S. Fery-Forgues, D. Lavabre, J. Chem. Educ. 76 (1999) 1260.
[34] J.R. Lakowicz, Principles of Fluorescence Spectroscopy, 2nd edn, Kluwer Academic/Plenum Publishers, New York, 1999.
[35] R.F. Kubin, A.N. Fletcher, J. Lumin. 27 (1982) 455.
[36] J. Rose, Advanced Physico-chemical Experiments, 1st edn, Sir Isaac Pitman and Sons Ltd., London, 1964, 257.
[37] A.L. Spek Platon, A Multipurpose Crystallographic Tool, Utrecht University, Utrecht, The Netherlands, 2001.
[38] B.D. Cullity, Elements of X-ray Diffraction, A.W.P.C. Inc., Massachusetts,1967.
[39] W.W. Yu, L. Qu, W. Guo, X. Peng, Chem. Mater. 15 (2003) 2854.
[40] F. Seker, K. Meker, T.F. Kuech, A.B. Ellis, Chem. Rev. 100 (2000) 2505.
[41] Y. Wang, Z. Tang, M.A. Correa-Duarte, I. Pastoriza-Santos, M. Giersig, N.A. Kotov, L.M. Liz-Marzan, J. Phys. Chem. B 108 (2004) 15461.
[42] Y. Yu, Y. Lai, X. Zheng, J. Wu, Z. Long, C. Liang, Spectrochim. Acta: A 68 (2007) 1356.
[43] M. Balsera, J.B. Arellano, F. Pazoz, D. Devos, A. Valencia, J. De Las Rivas, Eur. J. Biochem. 270 (2003) 3916.
[44] M. Guo, J.W. Zou, P.G. Yi, Z.C. Shang, G.X. Hu, Q.S. Yu, Anal. Sci. 20 (2004)465.